Development of a XY θ_z 3-DOF nanopositioning stage with linear displacement amplification device

Chih-Liang Chu[1,*], *Hung-Chi* Chen[1], and *Ming-Han* Sie[1]

[1]Department of Mechanical Engineering, Southern Taiwan University of Science and Technology, Tainan, Taiwan, R.O.C.

Abstract. The main purpose of this study is to develop a $XY\theta_Z$ 3-DOF nanopositioning stage with linear displacement amplification device. This stage is used by three groups of linear displacement amplification device to composition, and thus achieves precise $XY\theta_Z$ 3-DOF movement. The linear displacement amplification device makes use of a symmetrical layer mechanism, toggle amplification mechanism and parallel guiding spring to composition, and with amplification capability. Then it uses an equilateral triangle way to set the three groups of linear displacement amplification device. Overall design uses the finite element software ANSYS 12.0 to analysis the displacement, stress and dynamic response of nanopositioning stage. Experiment demonstrated takes the laser interferometer as the standard of displacement measurement. The result of experiment measurement shows that the maximum XY axis displacement and θ_Z rotational angle travel of the stage is 36.5μm, 32μm and 265 arc sec.

1 Introduction

In recent years, nanopositioning has become a key technology within many fields, including electron microscopy and x-ray lithography. These fields have an increasing demand for precision positioning systems capable of providing a wide operating range with high-accuracy and nanometer scale resolution, and minimum lateral and tilting motion. Therefore, developing systems that achieve precise positioning with a nanometer scale resolution has become a crucial requirement if highly precise micro-applications are to be developed.

When developing high-precision positioning mechanisms, it is common to employ piezoelectric actuators, which are capable of providing highly accurate nanoscale displacements. The stack-piezoelectric actuator effect produces an internal material twisting piezoelectric effect, which enables incremental displacements with a very high level of accuracy, delivers a high-resolution displacement output, provides a huge motive force, yields an efficient response, and enables a high mechanical switching efficiency. However, the displacement output of the piezoelectric actuator is limited, and consequently it is frequently necessary to adopt some form of amplification arrangement to extend its range. The displacement resolution of the actuator is further enhanced by means of a flexure hinge, which eliminates friction during mechanical motion of the actuator, and hence prevents undesirable heating effects.

Positioning systems play a fundamental role within nanotechnology applications, and therefore they are attracting an ever-increasing amount of interest within academic circles and in a variety of research units [1-9]. Physic Instrumente [10] provides products of nanopositioning stages to meet different applications. Xu and King [11] studied aspects of the design of flexure hinges for piezoactuator displacement amplifiers. Chang and Du [12] adopted the traditional Scott-Russell's straight-line mechanism method in developing a nanopositioning stage. In their design, a series connection method was employed to combine two Scott-Russell mechanisms in order to amplify the displacement output. In their device, the displacement output caused movement of a parallel guide spring, and it was shown that the straight line and angular deviation were minimized successfully. Their results indicated that the device was capable of a dynamic displacement in excess of 100 μm with a displacement resolution of 0.04 μm and an angular deviation of 31.1 μrad.

Ryu, Gweon, and Moon [13] successfully developed a $XY\theta_z$ micro-movement positioning stage. The stage uses three piezoelectric actuators and a monolithic flexure hinge mechanism, which is designed to provide large θ motion. Their study also provided an excellent source of reference for each of the elements of the stage. The micro-movement positioning stage provided displacements of 41.5 μm and 47.8 μm in the x- and y-directions, respectively, and demonstrated a yaw motion of approximately 322.8 arcsec.

When using a layer mechanism as the amplification device for a positioning stage, the greater the magnitude of the lateral offset error, the greater the angular deviation caused by the layer effect, and the greater the difference of the lateral deviation. Therefore, the present study develops a positioning stage that employs a stack-piezoelectric actuator, a flexure hinge, a layer mechanism, a toggle amplification mechanism, and a

* Corresponding author: cliang@stust.edu.tw

guide device. The aims of this study are to design and fabricate a XYθ_z 3-DOF nanopositioning stage with linear displacement amplification device.

2 Design principle

As shown in Fig. 1, the adoption of a layer mechanism in the conventional positioning stage will result in a lateral offset. A piezoelectric actuator input force of F results in a lateral offset displacement of Δ_X at the output end, which induces an error, and hence indirectly affects the accuracy of the device.

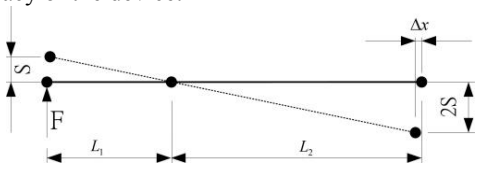

Fig. 1. A schematic drawing of a layer mechanism.

Fig. 2 presents a typical toggle amplification mechanism, in which A is the input and C is the output. When the toggle amplification mechanism is displaced, a lateral offset error is caused at the output end. For an input displacement of A_X, it is straightforward to determine the offset of the output. It is noted that the greater the layer angle, the greater the lateral offset of the output, and hence the greater the error. In the traditional design, two piezoelectric actuators are employed to simultaneously push the toggle amplification mechanism from either end in order to reduce the lateral offset error. However, this approach is not only more expensive, but also actually increases the lateral offset error because of the two different actuator forces.

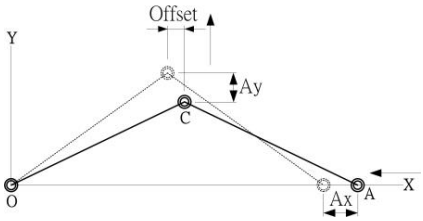

Fig. 2. A schematic demonstration of single direction input toggle amplification mechanism.

To overcome these limitations, the present study develops the positioning stage presented in Fig. 3. The proposed design combines the layer mechanism and a toggle amplification mechanism, and requires only one stack-piezoelectric actuator to supply the necessary driving input. When an electrical voltage is applied to the actuator, the corresponding length expansion, d_p, undergoes the first stage of amplification via a layer mechanism. Subsequently, the lateral offset of the layer mechanism is supplied as the input to the toggle amplification mechanism, where the second displacement amplification process is then performed. This two-step approach enables the lateral offset error caused by the layer mechanism amplification stage to be eliminated, and provides a two-stage displacement amplification function, hence increasing the output displacement of the positioning stage. Finally, the proposed design employs a 120° flexible pivot in order to ensure a precise straight-line displacement output.

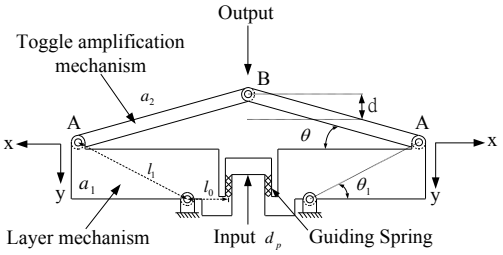

Fig. 3. A schematic demonstration of linear displacement amplification device [14].

From a rigid-body motion analysis of the proposed design, it can be shown that the relationship between the final output displacement and the amplification is given by:

$$d = a_1(\cos\theta_1 + a_2 \sin\theta_1)d_p \quad (1)$$

where $a_1=l_1/l_0$ is the amplification of the layer mechanism, $a_2=1/\tan\theta$ is the amplification of the toggle, d_p is the actuator input displacement, and d is the final output displacement.

An illustration of the develop linear displacement amplification device is presented in Fig. 4. The motion of the components in the linear displacement amplification device is described as follows. The length of the piezoelectric actuator, component 1, changes due to the driving voltage between the electrodes of the piezoelectric actuator. This length change pushes or pulls the input terminal of the layer mechanism, component 3, and causes displacements of the output terminal of the mechanism. The toggle amplification mechanism, component 4, is driven by the output displacements of component 3. Finally, the platform, component 7, moves due to the output motion of the flexible pivot, component 5. The parallel guide spring, component 6, joined to the platform can offer reaction force to prevent the platform from rotating and moving laterally.

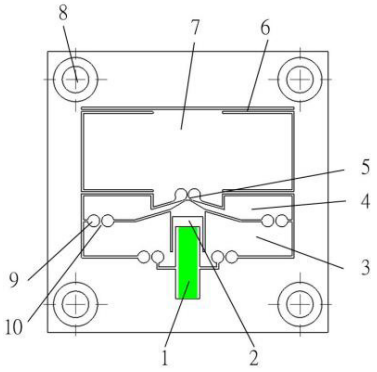

1. piezoelectric actuator, 2. layer guiding device, 3. layer mechanism, 4. toggle amplification mechanism, 5. flexible pivot, 6. parallel guide spring, 7. platform, 8. fixed screw holes, 9. cut-out slot to form flexure hinges, 10. flexure hinges.

Fig. 4. Schematic representation of the linear displacement amplification device.

Then use an equilateral triangle way to set the three groups of linear displacement amplification device presented in Fig. 5. This $XY\theta z$ 3-DOF nanopositioning stage by three groups of linear displacement amplification device to composition, and thus achieve X, Y, θ_z movement presented in Fig. 6.

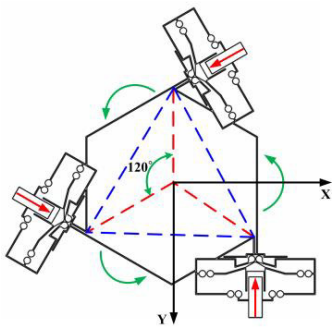

Fig. 5. Design schematic of the $XY\theta_z$ 3-DOF nanopositioning stage.

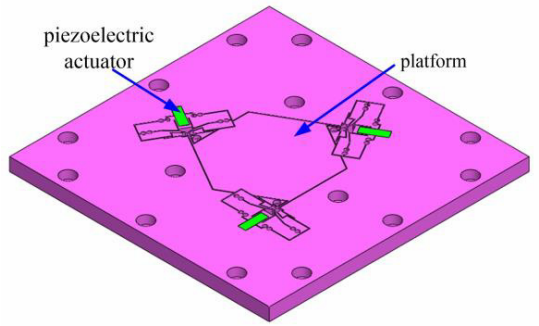

Fig. 6. Overall schematic of the $XY\theta_z$ 3-DOF nanopositioning stage.

3 Analysis and simulation

This study used the finite element method to develop the mathematical model of the stage, and then ANSYS software to simulate its operation. The design presented above was first modelled with limited elements. The simulation model adopted 20-nodes solid tetrahedron elements, SKD11 model steel as the structure material, and a structure thickness of 10mm. The Young's modulus was specified as $207\times10^9 N/m^2$, and the Poisson's ratio as 0.35. The simulation results are presented in Fig. 7.

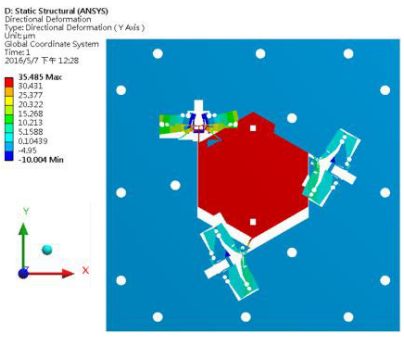

(a) X-axis displacement movements.

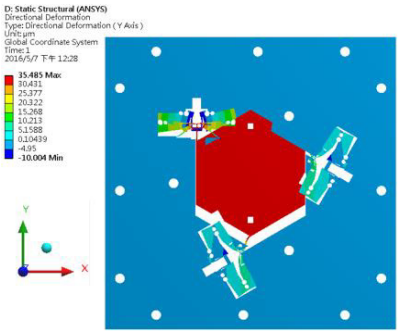

(b) Y-axis displacement movements

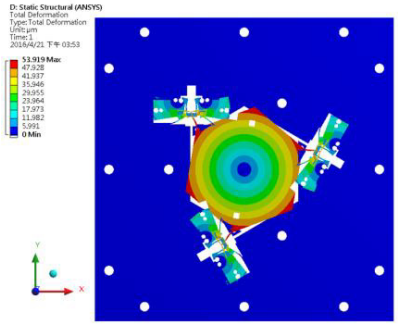

(c) θ_z-axis displacement movements

Fig. 7. ANSYS simulation result.

In the simulation process, a piezoelectric actuator input of 10μm was applied. This resulted in an output displacement of $XY\theta_z$ is 40.7μm, 35.4μm and 294.5 arcsec.

From the dynamic analysis presented in Fig. 8, it can be determined that the first natural frequency is 348.63 Hz, the second natural frequency is 349.34 Hz, and third natural frequency is 565.54 Hz. Analysis reveals that the stage is achieve $XY\theta_z$ 3-DOF movement.

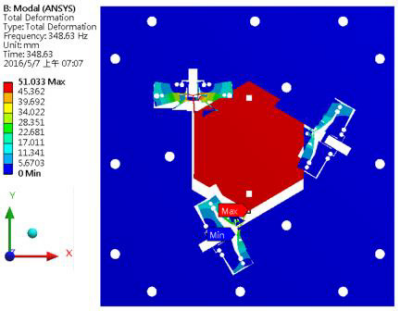

(a) The first natural frequency.

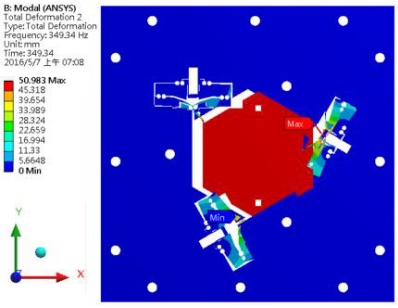

(b) The second natural frequency.

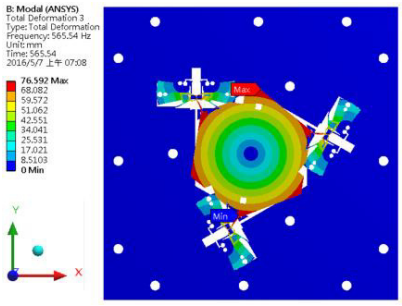

(c) The third natural frequency.

Fig. 8. ANSYS simulation results.

4 Experimental measurement

A precise Electro-Discharge Machining (EDM) process was used to fabricate the steel prototype (200mm×200mm×10mm) shown in Fig. 9. The corresponding engineering drawings were developed using solid modelling CAD software and then converted to DXF files as an input to the EDM machining. During the EDM process, all of the components were machined to a tolerance of ±5 μm.

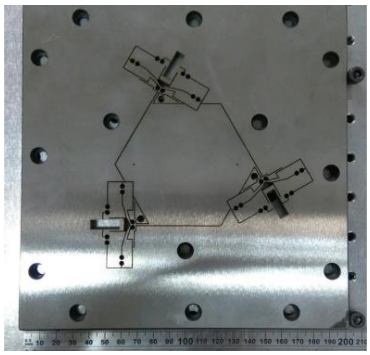

Fig. 9. Photograph of the nanopositioning stage.

Following assembly of the positioning stage, the piezoelectric actuator was installed at the pre-specified position and a series of experimental measurement tests were conducted in order to verify the functions of the stage and to determine its movement characteristics. The piezoelectric actuator, having a size of 5mm×5mm×18mm, is capable of travelling 20um and generating a force of 1800 N at 150 V [15].

As shown in Fig. 10, a non-contact laser interferometer (optodyne, model number MCV-500) with a resolution of 10 nm was used to investigate the performance of the stage. A mirror was attached to the movable stage such that the interferometer could detect the displacement of the stage as it was driven by the actuator. The function generator and a personal computer with a programmable AD/DA card were used to generate the desired waveform signal for testing the stage. The signals generated by the function generator or personal computer were amplified by a power amplifier to drive the piezoelectric actuator installed in the stage. The oscilloscope and personal computer were used to display, store, and analyse the experimental results in both time and frequency domains. The tested stage was placed on an air-bearing supported optical table and isolated from external vibrations.

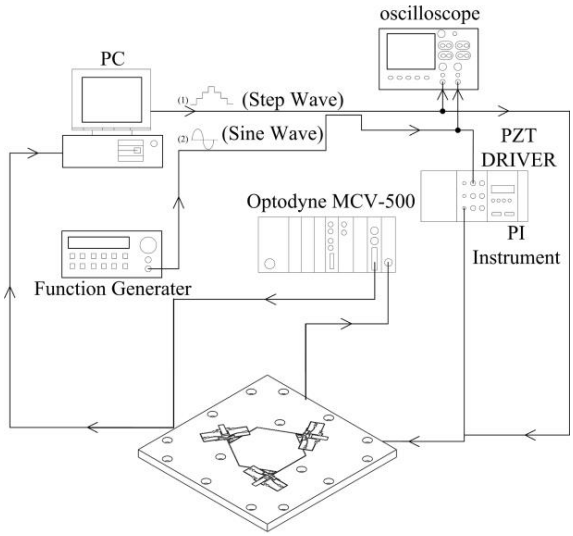

Fig. 10. Experiment set up flow chart.

4.1 Measurement of output displacement

To measure the XY-axis liner displacement, the mirror was initially located at the middle of the stage, as shown in Fig. 11. A voltage waveform was then applied, and the corresponding displacements measured by the laser interferometer. The mirror was positioning to a distance more than δ_x from the middle of the stage. Therefore, the maximum XY-axis liner displacement measurement was obtained for travel in both directions, and the straightness was then determined. Fig. 12, 13, 14 and 15 reveal that the X-axis liner displacement is 36.5 μm, the Y-axis liner displacement is 32 μm, and the XY-axis straightness is 0.3μm and 0.2μm.

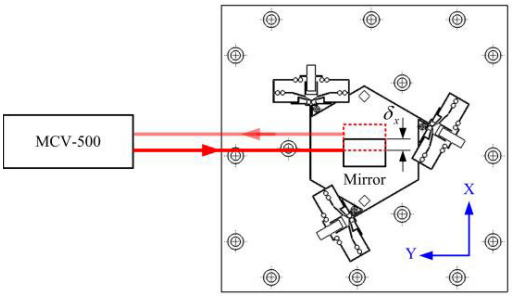

Fig. 11. Experimental arrangement for XY-axis liner displacement.

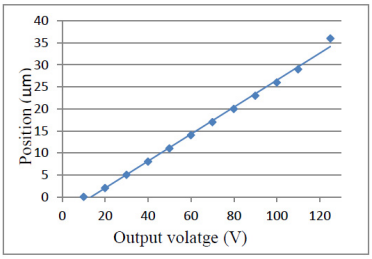

Fig. 12. X-axis liner displacement.

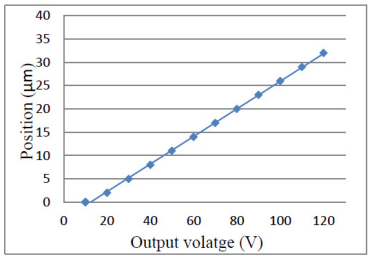

Fig. 13. Y-axis liner displacement.

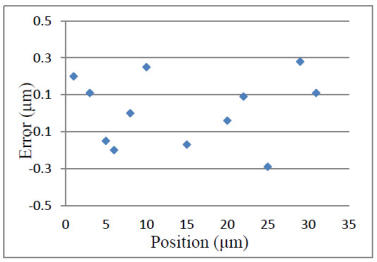

Fig. 14. X-axis straightness.

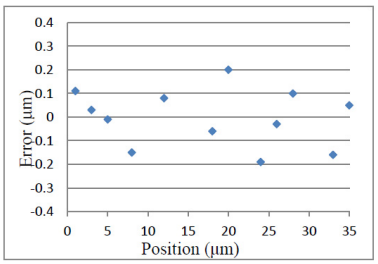

Fig. 15. Y-axis straightness.

To measure the θ_Z rotary displacement, the mirror was initially located at a distance more than 20 mm from the middle of the stage to the right side, as shown in Fig. 16. A voltage waveform was then applied, and the corresponding displacements measured by the laser interferometer. The mirror was then relocated to the symmetric position of the left side of the stage, and the experimental procedure was repeated. Hence, the maximum θ_Z rotary displacement measurement was obtained for travel in θ_Z directions. Fig. 17 and 18 reveal that the θ_Z rotary displacement is 265 arcsec, and that the θ_Z rotary angular error is ±10 arcsec.

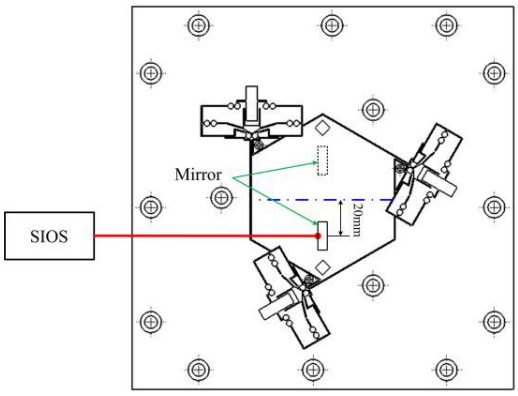

Fig. 16. Experimental arrangement for θ_Z rotary displacement.

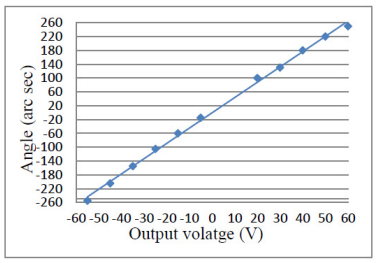

Fig. 17. θ_Z rotary displacement.

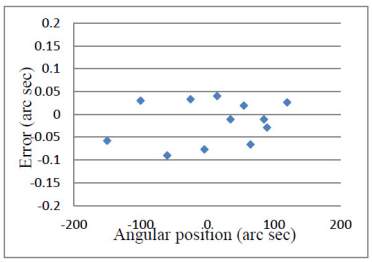

Fig. 18. θ_Z rotary angular error.

4.2 Frequency analysis

For a precision positioning device, a wide dynamic operating range is needed. Fig. 19 presents a schematic illustration of the experimental arrangement employed to analyse the frequency response of the proposed stage. An FTT Analyser (B&K, model 3560C) provided a sweep sinusoidal signal, which was amplified by the PI Instrument controller and then used to drive the piezoelectric actuator. An accelerometer was attached to the stage. Hence, providing the FFT Analyser with both the input signal of the piezoelectric actuator and the output signal of the accelerometer enabled the first natural frequency to be determined. As shown in Fig. 20, the first natural frequency is of the order of 349.8Hz, which is similar to the result obtained from the ANSYS analysis.

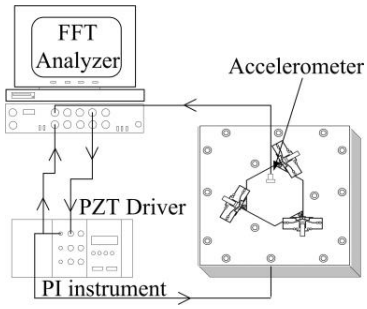

Fig. 19. Experimental arrangement for frequency analysis.

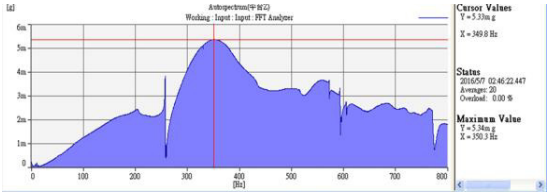

Fig. 20. The measured frequency response function of the nanopositioning stage.

5 Conclusion

This paper has presented the design and performance evaluation of a $XY\theta_z$ 3-DOF nanopositioning stage. The nanopositioning stage uses the minimum number of flexure hinges possible in order to reduce the angular elastic deformation. A layer mechanism is employed to provide the first stage of amplification, while the second amplification stage is provided by a toggle amplification mechanism, which eliminates the lateral offset effect of the preceding layer amplification.

The present experimental results have indicated that the θ_Z rotary displacement is 265 arcsec, that the θ_Z rotary angular error is less than ±10 arcsec, that the XY-axis liner displacement is approximately 36 μm, and that the XY-axis straightness is less than 0.3μm. Therefore, it has been demonstrated that the proposed $XY\theta_z$ 3-DOF nanopositioning stage.

Acknowledgement

The authors gratefully acknowledge the support to this project provided by the Ministry of Science and Technology, Taiwan, ROC under contract No. MOST 105-2622-E-218-009 -CC3 is gratefully acknowledged.

References

1. R. Yang, M. Jouaneh, R. Schweizer, Design and characterization of a low-profile micropositioning stage, *Precision Engineering*, **18**, 20-29 (1996)
2. F. E. Scire, E. C. Teague, Piezodrive 50-μm range stage with subnanometer resolution, *Rev. Sci. Instrum*, **42**, 1735-1740 (1978)
3. P. Gao, S. M. Swei, Z. Yuan, A new piezodriven precision micropositioning stage utilizing flexure hinge, *Nanotechnology*, **10**, 394-398 (1999)
4. S. H. Chang, C.K. Tseng, H. C. Chien, An Ultra-precision $XY\theta_Z$ Piezo-micropositioner-Part I: Design and Analysis, *IEEE Trans. Ultrasonics, Ferroelectrics, and Frequency Control*, **46**, 897-905 (1999)
5. S. H. Chang, C. K. Tseng, H. C. Chien, An Ultra-precision $XY\theta_Z$ Piezo-micropositioner-Part II: Experiment and Performance, *IEEE Trans. Ultrasonics, Ferroelectrics, and Frequency Control*, **46**, 897-905 (1999)
6. S. Yuki, P. Yuxin, K. Junji, A. Toyohiro, I. So, G. Wei, F.L. Tien, Design and construction of the motion mechanism of an XY micro-stage for precision positioning, *Sensors and Actuators A: Physical*, **201**, 395-406 (2013)
7. H. Tang, Y. Li, Design, analysis, and test of a novel 2-DOF nanopositioning system driven by dual mode, *IEEE Trans Robot*, **29**, 650-662 (2013)
8. L. Jianping, Z. Hongwei, Q. Xingtian, X. Z. Han Qu, F. Z. M. Zunqiang, F. Haishuang, Development of a compact 2-DOF precision piezoelectric positioning platform based on inchworm principle, *Sensors and Actuators A: Physical*, **222**, 87-95 (2015)
9. C. Leon, S. Bijan, B. Umesh, S. Julian, Z. Yongmin, Development and control of a two DOF linear–angular precision positioning stage, *Mechatronics*, **32**, 34-43 (2015)
10. Products for nanopositioning, Product Catalog of Physik Instrumente.
11. W. Xu, T. King, Flexure hinges for piezoactuator displacement amplifiers: flexibility, accuracy, and stress considerations, *Precision Engineering*, **19**, 4-10 (1996)
12. S. H. Chang, B. C. Du, A precision piezodriven micropositioner mechanism with large travel range, *Rev. Sci. Instrum*, **69**, 1785-1791 (1998)
13. J. W. Ryu, D. G. Gweon, K. S. Moon, Optimal design of a flexure hinge based $XY\theta_z$ wafer stage, *Precision Engineering*, **21**, 18-28 (1997)
14. C. L. Chu, S. H. Fan, A novel long-travel piezoelectric-driven linear nanopositioning stage, *Precision Engineering: The Journal of the International Societies for Precision Engineering and Nanotechnology*, **30**, 85-95 (2006)
15. Piezoelectrical and electrostrictive stack actuators and ring actuators, Product Catalog of Piezomechanik